Pressure-induced spin reorientation in $La_{1.2}Sr_{1.8}(Mn_{1-y}Ru_y)_2O_7$ ($y=0$ and 0.075) single crystals

K. Mydeen,[1,2] S. Arumugam,[1] P. Mandal,[3,a)] A. Murugeswari,[1] C. Sekar,[4] G. Krabbes,[5] and C. Q. Jin[2]

[1]*Centre for High Pressure Research, School of Physics, Bharathidasan University, Tiruchirappalli 620 024, India*
[2]*Beijing National Laboratory for Condensed Matter Physics, Institute of Physics, Chinese Academy of Sciences, Beijing 100 080, China*
[3]*Saha Institute of Nuclear Physics, 1/AF Bidhannagar, Calcutta 700 064, India*
[4]*Department of Physics, Periyar University, Selam-636011, India*
[5]*Institute for Solid State and Materials Research (IFW), D-01171, Dresden, Germany*

(Received 4 March 2009; accepted 1 October 2009; published online 17 November 2009)

The effect of hydrostatic pressure (P) and external magnetic field on the c-axis resistivity (ρ_c) and in-plane ac susceptibility (χ_{ab}) of $La_{1.2}Sr_{1.8}(Mn_{1-y}Ru_y)_2O_7$ ($y=0$ and 0.075) single crystals have been investigated. The ferromagnetic transition temperature (T_C) increases, while the conductivity decreases, with Ru doping. The application of pressure strongly decreases ρ_c and shifts T_C to higher temperature for both the samples. For the undoped ($y=0$) sample, T_C increases almost linearly with P up to 2 GPa, while T_C for the Ru-doped sample starts to saturate above 1.0 GPa. In the ferromagnetic state, the nature of P dependence of χ_{ab} of Ru-doped sample changes dramatically around 1.5 GPa. These results are explained by the pressure-induced spin reorientation from the basal plane to along the c-axis. © *2009 American Institute of Physics*. [doi:10.1063/1.3256158]

I. INTRODUCTION

Low-dimensional electronic and magnetic systems are of great interest for basic research as well as for technological applications. The discovery of colossal magnetoresistance (MR) in quasi-two-dimensional (quasi-2D) bilayer manganite $La_{2-2x}Sr_{1+2x}Mn_2O_7$ in which MnO_2 bilayers and $(La,Sr)_2O_2$ insulating rocksalt layers are stacked alternately, has drawn further attention in this field.[1–10] The presence of an insulating $(La,Sr)_2O_2$ layer in between MnO_2 conducting planes reduces interlayer coupling and, as a result, in-plane and out-of-plane transport and magnetic properties are highly anisotropic. Besides this, the coexistence of slowly fluctuating ferromagnetic (FM) and antiferromagnetic (AFM) microdomains, and the presence of short-range charge-orbital correlation in the paramagnetic (PM) state reduce the Curie temperature (T_C) for three-dimensional (3D) long-range spin ordering considerably.[8–10] Therefore, the T_C can be increased largely by suppressing these short-range correlations either by tuning the internal parameters such as carrier concentration (x) and impurity doping at Mn site or by applying external perturbation such as hydrostatic pressure. In contrast to 3D perovskite manganites, T_C of the present system does not increase significantly with carrier concentration. T_C increases only about 40 K over the whole range of doping $0.30 \leq x \leq 0.45$.[3] Several reports on Mn site substitution by $3d$ ions show that T_C decreases rapidly with increasing impurity concentration.[11–15] On the other hand, substitution of $4d$ Ru ion at Mn site appears to be quite exceptional.[16] Both metal-insulator transition (MIT) temperature (T_{MI}) and T_C increase, while the conductivity and saturated magnetization decrease, with Ru doping.[16,17] Moreover, Ru doping controls the easy axis of magnetization.[18] These features are ascribed to the strong uniaxial magnetic anisotropy of Ru ion and the AFM coupling between the Ru and Mn moments.[16–18]

Owing to the weak interlayer coupling and the large compressibility of the c-axis, external pressure is an important parameter for studying the variation in physical properties and T_C in bilayer manganites.[6] Often, the role of pressure on bilayer manganites is nontrivial and unexpected, and can be very different from that observed in 3D manganites.[2,19] In order to investigate the sensitivity of the electronic and magnetic properties on applied pressure, we present, in this paper, the results on the electrical resistivity and ac susceptibility of $La_{1.2}Sr_{1.8}(Mn_{1-y}Ru_y)_2O_7$ ($y=0$ and 0.075) single crystals as a function of temperature for different hydrostatic pressures in the presence of external magnetic fields (H). Though the transport and magnetic properties of pure sample ($y=0$) change systematically with P, the evolution of magnetic properties with P for Ru-doped sample is unusual and quite different from that of pure one. We observe that spin flips from in plane toward the c-axis with increasing P for Ru-doped sample, i.e., the easy axis of M changes from within the in plane to along the c-axis with the increase in P.

II. SAMPLE PREPARATION AND EXPERIMENTAL TECHNIQUES

Single crystals of nominal compositions $La_{1.2}Sr_{1.8}Mn_2O_7$ (LSMO) and $La_{1.2}Sr_{1.8}Mn_{1.85}Ru_{0.15}O_7$ (LSMRO) were grown from the polycrystalline rods using an image furnace in controlled atmosphere. Different experimental techniques were used to assess the phase purity, structure, and crystalline quality. The nature of the crystal surface was checked by optical and scanning electron microscopes. X-ray powder

a)Electronic mail: prabhat.mandal@saha.ac.in.

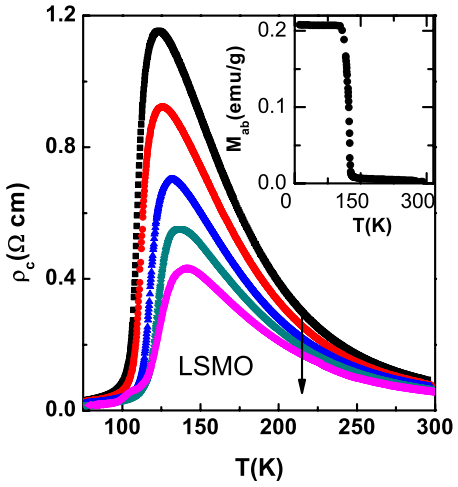

FIG. 1. (Color online) Temperature dependence of c-axis resistivity (ρ_c) for LSMO single crystal for different pressures (P). Inset: Temperature dependence of in-plane magnetization at H=0.01 T. The arrow indicates the direction of increase in P.

diffraction reveals high phase purity, and the sharp diffraction spots in Laue diffraction indicate high crystalline quality of the samples. The values of lattice parameters for LSMO are a=3.8725 Å and c=20.11 Å and the corresponding values for LSMRO are 3.8865 and 20.17 Å, respectively. These values of a and c are close to the lattice parameters reported for the oxygenated Ru-doped polycrystalline $La_{1.2}Sr_{1.8}(Mn_{1-y}Ru_y)_2O_7$ samples.[20] The elemental analysis was done using electron probe microanalysis and found to be very close to the starting composition. Well-characterized crystals were aligned with a goniometer using Laue diffraction and cut along the ab plane and c-axis according to the required dimensions for different measurements and polished. The magnetic properties were studied using a superconducting quantum interference device magnetometer (Quantum Design) and an ac susceptometer (Oxford Instruments) with a small dc or ac magnetic field applied parallel and perpendicular to the ab plane. The effect of hydrostatic pressure (up to 2 GPa) and magnetic field on electrical resistivity (ρ) and hydrostatic pressure on real part of in-plane ac susceptibility were measured in an Oxford Instruments Mag Laboratory EXA system with a self-clamp-type hybrid hydrostatic pressure cell, and the pressure was monitored using a manganin resistance device. The mixture of fluorinate FC70 and FC77 was used as a pressure transmitting medium. The values of different pressures that appear in this work refer to the values measured at room temperature. The temperature dependence of the electrical resistivity at ambient pressure was reproduced after releasing the pressure.

III. EXPERIMENTAL RESULTS

The temperature dependence of c-axis resistivity (ρ_c) for LSMO single crystal at various applied pressures is shown in Fig. 1. At ambient pressure, ρ_c increases rapidly with decreasing temperature until T_{MI} is reached below which ρ_c drops abruptly. Resistivity below T_{MI} drops by a factor of 15. With increasing P, ρ_c decreases and T_{MI} increases. It is clear from the figure that due to the sharp nature of MIT and its shift toward higher temperature with applied pressure, this system exhibits a large negative piezoresistance at T_{MI}. The effect of pressure on ρ_c is extended over a wide range of T above T_{MI}. However, the influence of pressure on the electrical resistivity is strongest in the vicinity of T_{MI}. The peak resistivity (ρ_p) at T_{MI} of $\rho_c(T)$ curve decreases almost exponentially with P. As MIT in manganites is accompanied by a FM to PM phase transition, we have also investigated the temperature dependence of magnetization. The inset of Fig. 1 shows the low-field in-plane magnetization $M_{ab}(T)$ curve for the LSMO single crystal at ambient pressure with H(=0.01 T) parallel to the ab plane. M_{ab} increases sharply at T_C and then starts to saturate with a further decrease in temperature. In the PM state, M_{ab} increases monotonically with decreasing temperature.

The temperature profile of ρ_c for LSMRO at different pressures is shown in Fig. 2(a). From Figs. 1 and 2, it is clear that T_{MI} increases, while the conductivity decreases, with Ru doping. T_{MI}(=144 K) for LSMRO is 21 K higher than that for LSMO at ambient condition. However, the sharpness of MIT is strongly reduced due to the appreciable increase in resistivity just below T_{MI}, with Ru doping. Ru doping enhances the charge localization phenomenon at low tempera-

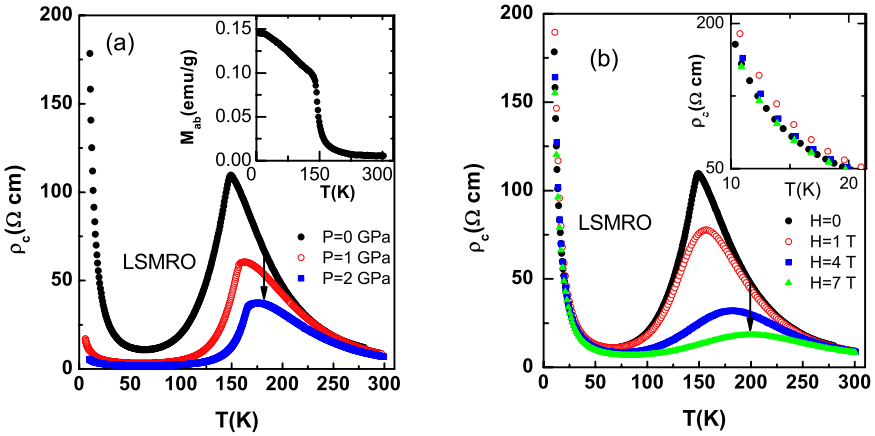

FIG. 2. (Color online) (a) Temperature dependence of c-axis resistivity (ρ_c) for LSMRO single crystal for different pressures (P). The inset shows the temperature dependence of in-plane magnetization at H=0.01 T. (b) Temperature dependence of ρ_c for LSMRO single crystal for different magnetic fields at ambient pressure. The inset shows T dependence of ρ_c below 20 K for different H. The arrows indicate the direction of increase in P and H.

ture too and, as a result, $\rho_c(T)$ curve exhibits a broad minimum at around $T_{SR}=65$ K. The pressure dependence of ρ_c for LSMRO is qualitatively similar to that for LSMO. ρ_c decreases with increasing pressure in the PM as well as in the FM states. However, the effect of P on ρ_c just below T_{MI} is stronger for LSMRO than that for LSMO. Due to this fact, the MIT becomes sharper with increasing pressure for LSMRO. Apart from this, pressure strongly suppresses the low-temperature resistivity upturn, whereas T_{SR} decreases slowly with increasing pressure. The inset of Fig. 2(a) shows the $M_{ab}(T)$ curve for LSMRO at $P=0$ and $H=0.01$ T. M_{ab} increases monotonically with decreasing T followed by a sharp increase at T_C. In the FM state too, M_{ab} continues to increase almost linearly with decreasing T without any sign of saturation down to 5 K and the value of M_{ab} is smaller than that for LSMO. Yu *et al.*[18] studied the temperature dependence of magnetization for samples with different Ru contents. They observed that M_{ab} decreases and the easy axis of magnetization changes with Ru doping. For $y=0.05$ and 0.075, the easy axis of magnetization changes from in plane to out of plane at $T_{SR}\sim 75$ K due to the spin reorientation. This temperature is close to the resistivity minimum for our $y=0.075$ sample. Thus we can attribute the relocalization of charge carriers at low temperature to spin-reorientation phenomenon.

For understanding the nature of charge localization at low temperature in LSMRO, we have studied the magnetic field dependence of resistivity at ambient pressure. The temperature dependence of ρ_c for different H is shown in Fig. 2(b). Similar to pressure, magnetic field strongly suppresses the resistivity both above and below T_{MI}. However, in the low-temperature region well below T_{MI}, where resistivity increases steeply with decreasing temperature, the effect of magnetic field on ρ_c is quite different. The inset of Fig. 2(b) shows the enlarged view of H dependence of ρ_c below 20 K. In contrary to pressure, ρ_c does not decrease monotonically with H. Initially, ρ_c increases with H up to a critical field and then decreases with further increase in H, i.e., a positive MR below the critical field. MR becomes slightly negative only at $H=7$ T. Positive MR has been observed in many strongly disordered materials and has been interpreted as a result of a decrease in the localization length induced by magnetic field.[21,22] The mechanisms through which P and H enhance charge conduction are not the same: H, favoring the spin alignment between neighboring Mn ions, enhances the bandwidth of e_g electrons and, therefore, the mobility via the double exchange mechanism. So, the effect of H on ρ_c will be significant in the vicinity of T_C but not at low temperature. On the other hand, P enhances the bandwidth directly by modifying the MnO bond length and Mn–O–Mn bond angle.[6,23] These structural variations that enhance electron hopping between Mn sites and suppress self-trapping energy of the carrier remain effective even at low temperature, i.e., an increase in conductivity with pressure.

The combined effect of pressure and magnetic field on the temperature dependence of ρ_c for LSMRO are shown in Figs. 3(a) and 3(b). These figures show that at a given P, ρ_c decreases and T_{MI} increases with increasing magnetic field as in the case of H dependence of ρ_c at ambient pressure [Fig. 2(b)]. In these cases also, the effect of magnetic field on ρ_c is stronger in the vicinity of T_{MI}. T_{MI} increases from 165 to 213 K at $P=1$ GPa and from 175 to 225 K at $P=2$ GPa as H increases from 0 to 5 T. At low temperature well below T_{MI}, ρ_c changes slowly with increasing H. Initially, ρ_c increases with H and then decreases with further increase in H for both $P=1$ and 2 GPa pressures. To understand the effect of pressure and magnetic field on resistivity of LSMRO more clearly, we have plotted the temperature dependence of MR defined as $\Delta\rho/\rho=[\rho(0)-\rho(H)]/\rho(0)$ for different H and applied pressures $P=0$, 1, and 2 GPa [Fig. 3(c)]. As expected, the largest negative MR is observed close to T_C but its value decreases on the both sides of T_C. From these figures, it is clear that the low-temperature MR is negative only when the strength of applied magnetic field exceeds a critical value.

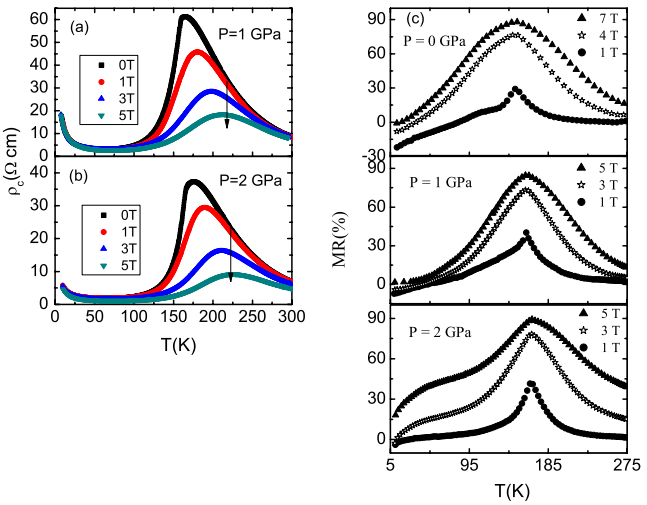

FIG. 3. (Color online) (a) Temperature dependence of c-axis resistivity (ρ_c) for LSMRO single crystal for different magnetic fields at $P=1$ GPa. (b) Temperature dependence of ρ_c for LSMRO single crystal for different magnetic fields at $P=2$ GPa. (c) Temperature dependence of MR of LSMRO single crystal for different magnetic fields H and applied pressures $P=0$ (upper panel), 1 GPa (middle panel), and 2 GPa (lower panel). The arrows in (a) and (b) indicate the direction of increase in H.

The temperature variation in the real part of in-plane ac magnetic susceptibility (χ_{ab}) of LSMO under different pressures is shown in Fig. 4(a). Similar to resistivity, $\chi_{ab}(T)$ curve shifts toward higher temperature with increasing P, i.e., T_C increases monotonically with P. The rapid increase in χ_{ab} at around T_{MI} indicates that MI and FM-PM transition temperatures are close to each other. In the PM state, χ_{ab} decreases monotonically with increasing T. The inset of Fig. 4(a) shows $\chi_c(T)$ of LSMO measured at ambient pressure. The temperature dependence of χ_c is very different from that of χ_{ab} in the PM state as well as in the FM state. In the PM state, χ_c is large and increases with decreasing temperature until T_C is reached. χ_c drops sharply at T_C and then increases slowly with further decreasing T. This indicates strong anisotropy in magnetic properties.

The main panel of Fig. 4(b) shows $\chi_{ab}(T)$ for LSMRO at different pressures up to 2 GPa and the inset shows $\chi_c(T)$ at ambient pressure. Both T and P dependences of χ_{ab} of LSMRO are very different from that of χ_{ab} of LSMO. For $P\leq 1.0$ GPa, the T dependence of χ_{ab} in the FM state is qualitatively similar to that of $M_{ab}(T)$ [inset of Fig. 2(a)]. On

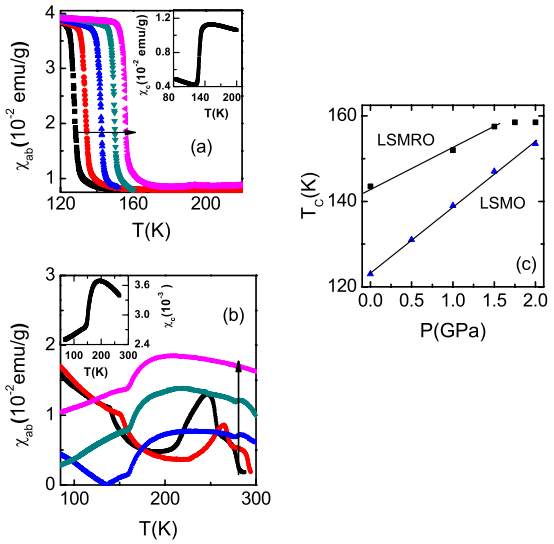

FIG. 4. (Color online) (a) Temperature dependence of in-plane ac susceptibility (χ_{ab}) for LSMO single crystal at P=0, 0.5, 1.0, 1.5, and 2.0 GPa. Inset: Temperature dependence of out-of-plane ac susceptibility (χ_c) at ambient pressure. (b) Temperature dependence of in-plane ac susceptibility (χ_{ab}) for LSMRO single crystal at P=0, 1.0, 1.5, 1.75, and 2.0 GPa. Inset: Temperature dependence of out-of-plane ac susceptibility (χ_c) at ambient pressure. (c) The pressure dependence of T_C for LSMO and LSMRO single crystals. The arrow indicates the direction of increase in P.

the other hand, χ_{ab} does not increase monotonically with decreasing T in the PM state as in the case of LSMO. χ_{ab} increases sharply at a temperature as high as T_{on}=278 K and then passes through a peak at T_p=244 K for P=0. With increasing P, both T_{on} and T_p increase and the peak becomes broad. For $P>1.0$ GPa, the nature of $\chi_{ab}(T)$ curve changes dramatically. Initially, χ_{ab} increases with T and then remains almost insensitive to T up to ~300 K. The temperature dependence of χ_{ab} above 1.5 GPa is qualitatively similar to that of χ_c at ambient pressure. The strong increase in χ_{ab} with pressure suggests that the magnetic transition below 300 K is intrinsic and might be due to the short-range magnetic ordering or due to the polaronic effect. It is clear from the figure that both temperature and pressure dependences of χ_{ab} for LSMRO in the FM state are not simple. In the low-pressure regime ($P \leq 1.0$ GPa), χ_{ab} increases monotonically with decreasing T. However, at high pressures $P>1.5$ GPa, χ_{ab} decreases with decreasing T. For P=1.5 GPa, χ_{ab} decreases as T decreases from T_C to 135 K and then increases with further lowering of T, i.e., $d\chi_{ab}/dT$ changes its sign at around 1.5 GPa. From the temperature dependence of χ_{ab} at different pressures, one can determine the dependence of χ_{ab} on P at a given T. This dependence will be useful to understand the evolution of magnetic properties with pressure and to determine the spin-flip pressure. Figure 4(b) shows that χ_{ab} slightly below T_C decreases with increasing P up to 1.5 GPa and then increases rapidly with further increase in P. Thus, from the dependence of χ_{ab} on T and P, we can say that there is a change in magnetic properties at around 1.5 GPa. For further understanding the role of pressure on electronic and magnetic properties, we have plotted the pressure dependence of T_C for LSMO and LSMRO samples in Fig. 4(c). T_C increases approximately linearly with P at the rate of 16 K/GPa for LSMO, while a strong departure from the linear behavior has been observed in LSMRO for $P>1$ GPa. Above 1 GPa, T_C increases slowly and saturates at 160 K. At this point, it may be interesting to compare the present result with that of T_C increase with Ru doping.[16,17] In this case also, initially T_C increases with Ru content and then starts to saturate at about 160 K for y=0.20, where the easy axis of magnetization becomes parallel to c-axis. Our study predicts that similar behavior may be observed in LSMO at high pressures above 2.5 GPa when T_C reaches ~160 K.

IV. DISCUSSION

The unusual behavior of ρ_c and χ_{ab} for LSMRO suggests that the magnetic structure of Ru-doped sample is strongly modified by the external pressure. Unlike in 3D perovskite manganites, the role of pressure on structural, magnetic, and transport properties of bilayer manganites is extremely sensitive to the hole concentration (x) and A-site ionic radius possibly due to the change in the orbital character of e_g conduction electron with doping.[2,24–26] It has been shown that with decreasing hole concentration, the c-axis increases and the orbital character of e_g electron changes from x^2-y^2 to $3z^2-r^2$ type and, as a consequence, the easy axis of M reorients from within the ab plane to along the c-axis.[3] Earlier results on $La_{2-2x}Sr_{1+2x}Mn_2O_7$ show that T_C depends linearly on P when spins are lying on the ab plane (x=0.40).[4] On the other hand, for x=0.32 in which spins are aligned along the c-axis, a large decrease in dT_C/dT is observed above a critical value of P_c~0.6 GPa due to the spin flop from the c-axis to the basal plane.[5] This suggests that the strong deviation from the linear increase in T_C with pressure at 1.5 GPa for LSMRO is possibly due to the change in the spin configuration. Thus, for understanding the role of pressure on magnetic structure of Ru-doped sample, we need to consider the orbital degrees of freedom of the e_g electrons. Structural and magnetic properties reveal that the apical MnO bond length increases monotonically with increasing Ru doping and the direction of easy axis of M changes from within the ab plane to along the c-axis above a critical value of Ru content (y=0.20), i.e., Ru doping stabilizes $3z^2-r^2$ orbital state of e_g electron.[18,20] So, one can increase the occupation number of $3z^2-r^2$ orbital either by reducing the hole concentration or by doping Ru at Mn site. This unique behavior of M in Ru-doped sample may be attributed to the magnetic anisotropy of Ru ion and the AFM coupling between the Mn and Ru spins.[16–18] Also, Hao and Wang showed that the occupation number of $3z^2-r^2$ orbital can be increased further by applying hydrostatic pressure.[26]

In this section, we try to analyze the effect of pressure on the spin-reorientation phenomenon in Ru-doped sample. The change in easy axis of magnetization and the suppression of T_{SR} may be understood from the random walk theory which yields a relation between the local anisotropy constants k_i, the relative magnetization (M/M_s), and the macroscopic anisotropy constants K_i, including phonon- and spin-orbit interactions:[27–29]

$$K_i(T) = k_{\text{ieff}}[1 - \alpha(p)(T/T_C)](M/M_s)^n, \quad (1)$$

where k_{ieff} is a combination of local anisotropy constants, n is an exponent, and α is a coefficient. The coefficient α should be sensitive to all external parameters that change the lattice volume.[30] In the simplest case, α is the thermal expansion coefficient. The spin-reorientation temperature is given by $T_{\text{SR}}=T_C/\alpha$. So, T_{SR} may be well pressure dependent. Now we can connect the spin reorientation with the carrier relocalization phenomenon at low temperatures. For a linear approximation $\alpha(p)=\alpha(0)(1+ap)$, we have $T_{\text{SR}}=[T_C/\alpha(0)](1-ap)$, for $a \ll 1$. Thus we obtain a spin-reorientation temperature which goes down with increasing pressure (Fig. 2), while T_C increases with the pressure (Fig. 4).

V. CONCLUSIONS

In conclusion, the influence of hydrostatic pressure (P) on transport and magnetic properties of LSMO and LSMRO single crystals has been studied systematically. The application of pressure strongly enhances the conductivity and T_C for both the samples. Our measurements clearly show that the effect of external pressure on magnetic and electrical properties of Ru-doped sample is quite different from that of LSMO. T_C increases almost linearly with P up to 2 GPa for LSMO, while T_C for the Ru-doped sample starts to saturate above 1.0 GPa. In the FM state, the nature of P dependence of χ_{ab} for LSMRO changes dramatically above 1 GPa. These unusual behavior of magnetic properties of LSMRO are due to the change in the orientation of the ordered spins from the basal plane to the c-axis with increasing P, i.e., pressure-induced shift of spin-reorientation transition.

ACKNOWLEDGMENTS

This research work was supported by the Third World Academy of Sciences, Italy, and Chinese Academy of Sciences, People's Republic of China for the award of CAS-TWAS fellowship. S.A. would like to thank DST, UGC and CSIR, New Delhi for financial support.

[1]T. Kimura, Y. Tomioka, H. Kuwahara, A. Asamitsu, M. Tamura, and Y. Tokura, Science **274**, 1698 (1996).
[2]T. Kimura, A. Asamitsu, Y. Tomioka, and Y. Tokura, Phys. Rev. Lett. **79**, 3720 (1997).
[3]T. Kimura, Y. Tomioka, A. Asamitsu, and Y. Tokura, Phys. Rev. Lett. **81**, 5920 (1998).
[4]J.-S. Zhou, J. B. Goodenough, and J. F. Mitchell, Phys. Rev. B **58**, R579 (1998).
[5]J.-S. Zhou, J. B. Goodenough, and J. F. Mitchell, Phys. Rev. B **61**, R9217 (2000).
[6]D. N. Argyriou, J. F. Mitchell, J. B. Goodenough, O. Chmaissem, S. Short, and J. D. Jorgensen, Phys. Rev. Lett. **78**, 1568 (1997).
[7]S. Arumugam, K. Mydeen, N. Manivannan, M. K. Vanji, D. Prabhakaran, A. T. Boothroyd, R. K. Sharma, and P. Mandal, Phys. Rev. B **73**, 212412 (2006).
[8]T. G. Perring, G. Aeppli, Y. Moritomo, and Y. Tokura, Phys. Rev. Lett. **78**, 3197 (1997).
[9]L. Vasiliu-Doloc, S. RosenKranz, R. Osborn, S. K. Sinha, J. W. Lynn, J. Mesot, O. H. Seeck, G. Preosti, A. J. Fedro, and J. F. Mitchell, Phys. Rev. Lett. **83**, 4393 (1999).
[10]T. Ishikawa, K. Tobe, T. Kimura, T. Katsufuji, and Y. Tokura, Phys. Rev. B **62**, 12354 (2000).
[11]R. Gundakaram, J. G. Lin, F. Y. Lee, M. F. Tai, C. H. Shen, R. S. Liu, and C. Y. Huang, J. Phys.: Condens. Matter **11**, 5187 (1999).
[12]J. Zhang, Q. Yan, F. Wang, P. Yuan, and P. Zhang, J. Phys.: Condens. Matter **12**, 1981 (2000).
[13]K. B. Chashka, B. Fisher, J. Genossar, A. Keren, L. Patlagan, and G. M. Reisner, Phys. Rev. B **65**, 134441 (2002).
[14]H. Zhu, X.-M. Liu, K.-Q. Ruan, and Y.-H. Zhang, Phys. Rev. B **65**, 104424 (2002).
[15]M. Matsukawa, M. Chiba, E. Kikuchi, R. Suryanarayanan, M. Apostu, S. Nimori, K. Sugimoto, and N. Kobayashi, Phys. Rev. B **72**, 224422 (2005).
[16]F. Weigand, S. Gold, A. Schmid, J. Geissler, and E. Goering, Appl. Phys. Lett. **81**, 2035 (2002).
[17]Y. Onose, J. P. He, Y. Kaneko, T. Arima, and Y. Tokura, Appl. Phys. Lett. **86**, 242502 (2005).
[18]X. Z. Yu, M. Uchida, Y. Onose, J. P. He, Y. Kaneko, T. Asaka, K. Kimoto, Y. Matsui, T. Arima, and Y. Tokura, J. Magn. Magn. Mater. **302**, 391 (2006).
[19]J. J. Neumeier, M. F. Hundley, J. D. Thompson, and R. H. Heffner, Phys. Rev. B **52**, R7006 (1995); I. V. Medvedeva, Y. S. Bersenev, K. Bärner, L. Haupt, P. Mandal, and A. Poddar, Physica B **229**, 194 (1997); J. Fontcuberta, V. Laukhin, and X. Obradors, Appl. Phys. Lett. **72**, 2607 (1998); K. Mydeen, P. Sarkar, P. Mandal, A. Murugeswari, C. Q. Jin, and S. Arumugam, *ibid.* **92**, 182510 (2008).
[20]B. Schüpp, K. Dörr, K. Ruck, K. Nenkov, K. -H. Müller, and G. Krabbes, Solid State Sci. **7**, 17 (2005).
[21]W. Jiang, J. L. Peng, J. J. Hamilton, and R. L. Greene, Phys. Rev. B **49**, 690 (1994); P. Mandal, A. Neumann, A. G. M. Jansen, P. Wyder, and R. Deltour, *ibid.* **55**, 452 (1997); P. Mandal, A. Hassen, and A. Loidl, *ibid.* **69**, 224418 (2004); K. Bärner, P. Mandal, and R. von Helmolt, Phys. Status Solidi B **223**, 811 (2001).
[22]B. I. Shklovskii and B. Z. Spivak, in *Hopping Transport in Solids*, edited by M. Pollak and B. I. Shklovskii (Elsevier Science, Vancouver, 1991).
[23]C. Meneghini, D. Levy, S. Mobilio, M. Ortolani, M. Nuñez-Reguero, A. Kumar, and D. D. Sarma, Phys. Rev. B **65**, 012111 (2001); V. Laukhin, J. Fontcuberta, J. L. García-Múñoz, and X. Obradors, *ibid.* **56**, R10009 (1997).
[24]K. V. Kamenev, M. R. Lees, G. Balakrishnan, D. McK. Paul, W. G. Marshall, V. G. Tissen, and M. V. Nefedova, Phys. Rev. Lett. **84**, 2710 (2000).
[25]K. V. Kamenev, G. J. McIntyre, Z. Arnold, J. Kamarád, M. R. Lees, G. Balakrishnan, E. M. L. Chung, and D. McK. Paul, Phys. Rev. Lett. **87**, 167203 (2001).
[26]L. Hao and J. Wang, Phys. Rev. B **76**, 134420 (2007).
[27]C. Zener, Phys. Rev. **96**, 1335 (1954).
[28]W. F. Carr, Phys. Rev. **109**, 1971 (1958).
[29]R. Brenner, Phys. Rev. **107**, 1539 (1957).
[30]H. J. Kohnke, V. Dankelman, N. C. H. Kleeberg, J. W. Schunemann, K. Bärner, A. Vetcher, and G. A. Govor, Phys. Status Solidi B **191**, 511 (1995).